Journal of RADIATION INDUSTRY
Vol. 19, No. 3, pp. 209-219, 2025
https://doi.org/10.23042/radin.2025.19.3.209

Original article

Ionizing Radiation Increases Axl Protein Degradation in A549 Lung Adenocarcinoma Cells through an Autophagolysosomal Pathway

Hyo Jin Choi[1,†], Gyeong Han Jeong[2,†], Hanui Lee[2], Kon-Young Ji[3], Byung Yeoup Chung[2], Hyoung-Woo Bai[2,4,*], and Eun-Hee Lee[1,*]

[1]Medical Device Development Centrer, Daegu-Gyeongbuk Medical Innovation Foundation (K-MEDI hub), 80, Cheombok-ro, Dong-gu, Daegu 41061, Republic of Korea.
[2]Division for Biotechnology, Advanced Radiation Technology Institute (ARTI), Korea Atomic Energy Institute (KAERI), 29 Geumgu-Gil, Jeongeup-si, Jeollabuk-do 580-185, Republic of Korea
[3]Herbal Medicine Research Division, Korea Institute of Oriental Medicine, 1672 Yuseong-daero, Yuseong-gu, Daejeon 34054, Republic of Korea
[4]Radiation Biotechnology and Applied Radioisotope Science, University of Science and Technology (UST), Daejeon 34113, Republic of Korea

ABSTRACT Axl receptor tyrosine kinase (Axl) plays multiple roles in the tumorigenesis and metastasis of several cancers. Herein, we report that the degradation of Axl protein following ionizing radiation (IR) exposure is associated with the autophagolysosomal pathway in A549 lung adenocarcinoma cells. The level of Axl protein was markedly decreased after IR exposure to 5 or 10 Gy, although the Axl transcriptional level remained unaltered. IR-mediated Axl degradation was inhibited by the lysosomal inhibitor, chloroquine, whereas treatment with the proteasome inhibitors, MG132 and lactacystin, did not affect Axl degradation. Furthermore, the expression of Axl was correlated with increased cleavage of GFP-LC3-I to GFP-LC3-II (specific protein markers of autophagy) in IR treated cells compared to non-IR treated cells from 1-48 h after IR. Moreover, Axl co-localized with GFP-LC3 fusion protein in punctate spots, which are well-characterized markers of autophagosome formation, indicating that the IR-induced degradation of Axl protein is mediated by the autophagic process. Thus, our findings suggest that IR increases the degradation of Axl protein through the autophagolysosomal pathway and promotes the growth arrest of non-small cell lung cancer (NSCLC) cells.

Key words: Lung cancer, Ionizing radiation, Axl, Protein degradation pathway, Autophagolysosomal pathway

1. Introduction

Lung cancer is one of the most common types of cancer and a leading cause of cancer-related deaths[1]. Non-small cell lung cancer (NSCLC) accounts for up to 85% of all lung cancers [2]. Numerous scientific advances have been made in lung cancer diagnosis and treatment modalities over the past few decades, including surgery, chemotherapy, and radiotherapy [3]. Despite the use of these advanced therapies to increase the disease-free survival of lung cancer patients, many challenges still exist in the treatment lung cancer. The low sensitivity of NSCLC to chemo- and radiotherapy has been a major barrier to achieving a complete cure. Therefore, novel treatment approaches need to be developed for NSCLC.

The Axl receptor tyrosine kinase (Axl) is a member of the TAM (Tyro3-Axl-Mer) family of receptor tyrosine kinases (RTKs), that is overexpressed in different human cancers and enhances tumour progression [4,5]. Moreover, the expression of Axl has been shown to be correlated with drug resistance in patients with lung cancer, melanoma, myeloid leukaemia, and renal cell carcinoma [6-10]. Despite the rare expression in normal lung cells, a number of patients with NSCLC highly express Axl proteins, and Axl has been implicated in poorer prognosis, promotion of tumour growth, metastasis, and epithelial-mesen-

ISSN 1976-2402 http://www.ksri.kr/

Copyright© 2025 by Korean Society of Radiation Industry

*Corresponding authors
Hyoung-Woo Bai
Tel: +82-63-570-3388, Fax: +82-63-570-3339, E-mail: hbai@kaeri.re.kr
Eun-Hee Lee
Tel: +82-53-790-5597, Fax: +82-53-790-5519, E-mail: ehlee@kmedihub.re.kr
Received 9 June 2025 **Revised** 8 July 2025 **Accepted** 9 July 2025

chymal transition [11-15]. Therefore, considering its important role in NSCLC tumor growth, epithelial-mesenchymal transition (EMT), invasion, and drug resistance, Axl is a promising therapeutic target for NSCLC.

Ionizing radiation (IR) is the most commonly used treatment modality in lung cancer [16,17]. The high-energy radiation damages the cancer cells and thus inhibits their ability to proliferate further [18]. Recently, the radiation effects of cancer treatment have been explored widely in terms of radiation-induced cancer cell death and various cell signaling pathway associated with radiosensitivity, resistance, and molecular response to radiation [19-22]. Apoptotic cell death is known to be a primary mechanism of cell death in cancer cells following IR injury. The cell death following irradiation is preceded by cell cycle arrest at the G2/M phase, and some aberrant cells with incomplete mitosis undergo post-mitotic apoptosis [23,24]. In addition, the decrease in growth factors, generation of cellular reactive oxygen species (ROS), accumulation of modified proteins (oxidized and aggregated) and intracellular calcium, and ammonia also induce autophagy reaction [25]. In the stressful cellular conditions following IR, autophagy plays a crucial role in maintaining homeostasis in tumour cells [26].

Herein, we report a novel molecular mechanism by which Axl oncoprotein is degraded through autophagy in the A549 cells following IR injury. We found that the degradation of Axl protein in gamma-irradiated cells was inhibited by blockade of the autophagy pathway. Moreover, Axl protein co-localized in GFP-LC3 positive autophagosomes after IR. The results of our study provide insights into a novel mechanism in which IR plays a critical role in the autophagy-mediated downregulation of Axl protein expression in A549 tumour progression.

2. Methods

2.1. Cell lines, chemicals, and reagents

Human NSCLC, cell line A549 was obtained from the American Type Culture Collection (ATCC, Manassas, VA, USA). The A549 cells were grown in RPMI-1640 medium supplemented with 10% fetal bovine serum (FBS) at 37°C in a 5% CO_2 atmosphere. Chloroquine, lactacystin, and hydrogen peroxide were purchased from Sigma-Aldrich (St. Louis, MO, USA). Cycloheximide was obtained from A.G. Scientific (San Diego, CA, USA). MG132 was purchased from Cell Signaling Technology (Beverly, MA, USA). Immunoblot analyses were conducted using the following antibodies: anti-Axl (Santa Cruz Biotechnology, Santa Cruz, CA, USA); anti-ubiquitin, anti-LC3b, anti-GAPDH,anti-goat-HRP, anti-rabbit-HRP, and AlexaFluor 555 conjugated anti-goat antibody (Cell Signaling Technology, Beverly, MA, USA).

2.2. Gamma-irradiation

A549 cells were seeded at a density of 2.5×10^5 cells in 60-mm dishes in triplicate for 24 h prior to the irradiation. The plated cells without exposure to any radiation were used as control. The cells were brought to the irradiation facility to prevent variations in temperature, transport, and background irradiation. Cells were irradiated by IR with gamma-ray in a Gammacell 40 Exactor (MDS Nordion, Ottawa, Canada) at ARTI, KEARI, and exposed to a total dose of 5 and 10 Gy at a dose rate of 1.1 $Gy \cdot min^{-1}$. The cells were irradiated at room temperature (RT) in air. The irradiated and non-irradiated cells were further used for cell viability, cell cycle analysis, apoptotic assays, ROS detection assay, and immunoblot.

2.3. MTT assay for cell viability

The MTT assay was carried out as described previously [27]. A549 cells were trypsinized, made into a single cell suspension, and irradiated at different IR doses (5 and 10 Gy). The irradiated cells were seeded at a density of 5×10^3 cells per well in 96 well culture plates. After various time points (24, 48, 72, and 96 h), MTT (5 mg/mL in water; 20 μL/well) was added to the wells and incubated at 37°C for 4 h. The supernatant was removed and DMSO (100 μL/well) was added to dissolve the formazan formed in the wells. After shaking the plates, the cell viability in each well was measured with a microplate reader (Tecan, Männedorf, Switzerland) at 570 nm. The cell viability assay was performed in triplicate.

2.4. Cell cycle assay

After gamma-irradiation, the cells were harvested and fixed with 70% cold ethanol at –20°C for 24 h. For the cell cycle analysis, Muse™ Cell cycle reagent (EMD Millipore, Billerica, MA, USA) was used as previously described [28]. The fixed cells were washed twice with PBS and 150 μL of Muse™ cell cycle reagent was added. The cells were stained at RT for 30 min in the dark. For each sample, 10,000 events were collected, and flow cytometric analysis was performed by Muse™ Cell Analyser (EMD Millipore). The DNA contents are presented as the percentage of cells in the respective cell cycle phase detected using Muse 1.1.2 analysis software.

2.5. Annexin V apoptotic assay

For the quantitative analysis of apoptotic cells, Muse® Annexin V and Dead Cell Assay Kit (EMD Millipore) was used as previously described [27]. Briefly, the irradiated cells were harvested by trypsinization for analysis and washed with PBS followed by incubation with Annexin V/propidium iodide (PI) mixture in the binding buffer from the kit for 20 min at RT in the dark. Analysis of the apoptotic cells was performed by collecting 20,000 events and analyzed using Muse 1.1.2 analysis software.

2.6. Assessment of reactive oxygen species (ROS)

For the intracellular ROS accumulation assay, Muse® oxidative stress reagent assay kit (EMD Millipore) was used. Briefly, A549 cells (2.5×10^5) were seeded in 60-mm culture dishes for 24 h and then exposed to a total dose of 10 Gy gamma radiation. After 48 h, cells were harvested and incubated with the assay reagent for 30 min. Tert-butyl hydroperoxide (TBHP), a known inducer of oxidative stress, was used as a positive control. Cells were treated with 55 μM TBHP for 4 h at 37°C. Cells were harvested and stained with the assay reagent for 30 min. The stained cells were analyzed on the Muse™ Cell Analyser (EMD Millipore) according to the manufacturer's protocol.

2.7. Semiquantitative RT-PCR

Semiquantitative RT-PCR was performed as described previously [29]. The mRNA was isolated from A549 cells exposed to IR using the TRIzol reagent (Molecular Research Centre, Cincinnati, OH, USA). A total of 2 μg of mRNA was reverse transcribed using a GoScript complementary DNA (cDNA) Synthesis kit (Promega, Madison, WI, USA) to synthesize cDNA. The PCR reaction was performed using Emerald Amp PCR Master Mix (Takara, Otsu, Japan), according to the kit instructions. The resulting cDNA was amplified with the following primers: β-actin, 5′-GTGGGGCGCCCCAGGCACCA-3′ and 5′-CTCCTTAATGTCACGCACGAT-3′; Axl, 5′-CCC AGA ACC TGT GGT CAT CT-3′ and 5′-ACC GAG ACA TCA GGG CAT AC-3′.

2.8. Immunoblot analysis

Immunoblot analysis was performed as described previously [30]. Cells were washed twice with cold PBS and lysed in protein lysis buffer (Rockland, Limerick, PA, USA) for 30 min on ice, and the supernatant was collected. The protein concentration was measured using BCA assay, according to the manufacturer's instructions (Thermo Fisher Scientific, Seoul, Korea). Cell lysates containing equal amounts of protein (40 μg) were prepared and separated by 8-15% sodium dodecyl sulfate-polyacrylamide gel electrophoresis and transferred to polyvinylidene difluoride (PVDF) membranes (Merck Millipore, Billerica, MA, USA). The blot was incubated with blocking buffer (1% BSA and 5% skim milk in PBS) overnight at 4°C, and then washed three times with TBST (50 mM Tris pH 7.4, 150 mM NaCl, 0.05% Tween 20). The blot was probed with a primary antibody by incubation on a shaker at 4°C overnight and then incubated with the secondary antibody for 1 h at RT. After three washings in TBS, the signal was detected using the ECL system (GE Healthcare, Marlborough, MA, USA).

2.9. Immunofluorescence analysis

The cells were fixed in cold MeOH for 10 min. After three washes with PBS solution containing 4% FBS, the cells were permeabilized for 10 min with 0.1% Triton X-100 in PBS and then blocked with 5% BSA for 1 h. Cells were incubated overnight at 4°C with Axl antibody (1 : 500). The coverslips were washed with PBS, incubated 1 h at RT with AlexaFluor 555 conjugated anti-goat (1 : 1000 diluted) secondary antibody, and mounted with ProLong® with DAPI solution (Molecular Probe, Life Technologies, Carlsbad, CA, USA). Immunofluorescence images were acquired with a Zeiss LSM 800 confocal microscope with a 40x objective. The confocal images were analyzed using Zen image acquisition software (Carl Zeiss microscopy, Jena, Germany).

2.10. Plasmids and Transfection and fluorescence microscopy

A plasmid encoding pEGFP-LC3B construct (Addgene, plasmid 11546) was used for the quantification of autophagic maturation. Human Axl (NM_021913) open reading frame (ORF) was cloned into pDsRed2-N1 vector (Addgene, plasmid 632429) expression vector. Human Axl ORF was obtained from the pcDNA3.1-h.Axl expression vector [30]. Transiently transfected cells were generated by co-transfection with pEGFP-LC3B and pDsRed2-N1-h.Axl using the Amaxa Nucleofector device (Amaxa Inc., Gaithersburg, MD, USA). After 120 h, the transfected cells were exposed to gamma-rays. After 48 h of gamma-irradiation, the cells were treated with CQ for 3 h. The cells were fixed with 4% paraformaldehyde for 10 min. The fixed cells were prepared for fluorescence scanning. The images were captured with an Olympus IX71 fluorescence microscope (Olympus, Tokyo, Japan).

2.11. Statistical analysis

Statistical differences were evaluated using the Student's *t*-test. The results were considered statistically significant when *p*-values were <0.05. All experiments were performed at least three times independently.

3. Results

3.1. IR induces growth arrest and ROS accumulation in A549 cells

To determine the suppressive effects of IR on A549 lung adenocarcinoma cells, changes in cell proliferation were investigated after exposure to IR. As expected, the growth rate of A549 cells was significantly decreased following exposure to IR at 5 and 10 Gy in a time- and radiation dosage-dependent manner compared to control (Fig. 1A). Moreover, the exposure to IR induced the accumulation of ROS in A549 cells to a level similar to that observed in the positive control (TBHP treatment) (Fig. 1B). Given the suppressive effect of IR exposure on cell proliferation, the cell cycle was measured using flow cytometry. IR exposure for 24 and 48 h decreased the percentage of cells in S-phase and those arrested at the G2/M-phase of the cell cycle (Fig. 1C). Consistently, the percentage of apoptotic cells was slightly increased following IR exposure for 24 and 48 h (Fig. 1D). These results suggest that IR exposure induces growth arrest in lung adenocarcinoma cells through the suppression of cell cycle progression, and increased ROS accumulation.

3.2. IR enhances protein degradation of Axl in A549 cells

Given the inhibitory effect of IR on the proliferation of lung cancer cells, we examined whether IR modulated the expression of Axl. The gene expression of Axl did not change following the exposure of A549 cells to IR for 24 and 48 h (Fig. 2A, upper panel). Interestingly, the protein expression of Axl was down-regulated by the IR exposure at both 24 and 48 h (Fig. 2A, lower panel). To clarify the induction of Axl degradation following IR exposure, we investigated the protein expression of Axl in A549 cells after treatment with a protein synthesis inhibitor, cycloheximide (CHX). The half-life of Axl was approximately 30 min in A549 cells. Whereas the expression of Axl was observed to be about 30% in the control cells, following IR-treatment of the cells only about 10% of expression was detectable at 180 min (Fig. 2B). Therefore, we speculate that IR may be associated with Axl protein degradation, thereby affecting protein level without affecting Axl mRNA expression.

3.3. The proteasomal pathway is not involved in the degradation of the Axl protein

Generally, protein degradation is mediated through two major pathways; the proteasomal and lysosomal pathway [31]. To clarify the mechanism of the protein degradation of Axl following IR exposure in lung adenocarcinoma cells, we investigated the level of Axl protein in A549 cells after treatment with proteasomal or lysosomal inhibitors. To evaluate whether the proteasomal pathway was involved in Axl degradation, A549 lung cancer cells were treated with proteasomal inhibitors, lactacystin, and MG132. The protein expression of Axl was comparable between control and lactacystin-treated cells (Fig. 3A, lane 1 and 2), while it was slightly suppressed following MG132 treatment (Fig. 3A, lane 3). As expected, the protein expression of Axl was suppressed following H_2O_2-treatment which is capable of mimicking radiation effects (Fig. 3A, lane 4). However, the inhibitors could not retard the H_2O_2-induced Axl protein degradation (Fig. 3A, lane 5 and 6). To confirm the inhibitory effects of lactacystin and MG132 on the ubiquitin-proteasome pathway, the level of the accumulation of high-molecular-mass ubiquitin-proteins was analyzed by immunoblotting. The accumulation of high-molecular-mass ubiquitinated proteins was increased in both the single treatment with each inhibitor (Fig. 3B, lane 2 and 3) and in the co-treatment with H_2O_2 (Fig. 3B, lane 5 and 6) compared with control cells, respectively. The decreased protein level of Axl was not restored by treatment with lactacystin and MG132 in case of the inhibition of protein synthesis by CHX treatment and IR (Fig. 3C, D). Taken together, these findings demonstrate that the proteasome pathway is not involved in the IR-mediated Axl protein degradation in lung adenocarcinoma cells.

3.4. The autophagolysosomal pathway is involved in protein degradation of Axl in IR-induced A549 cells

Next, we used a lysosomal inhibitor, chloroquine (CQ), to determine whether the lysosomes were involved in the degradation of Axl protein. In contrast to the proteasome inhibitors, the H_2O_2-induced suppression of Axl protein level was restored by treatment with CQ (Fig. 4A). Likewise, the decreased level of Axl protein following inhibition of protein synthesis by CHX treatment was restored by treatment with CQ (Fig. 4B-D). Furthermore, the induction of Axl degradation following IR exposure was retarded by treatment with CQ (Fig. 4E). Taken together, these findings demonstrate that IR exposure promotes the Axl protein degradation of lung adenocarcinoma cells through

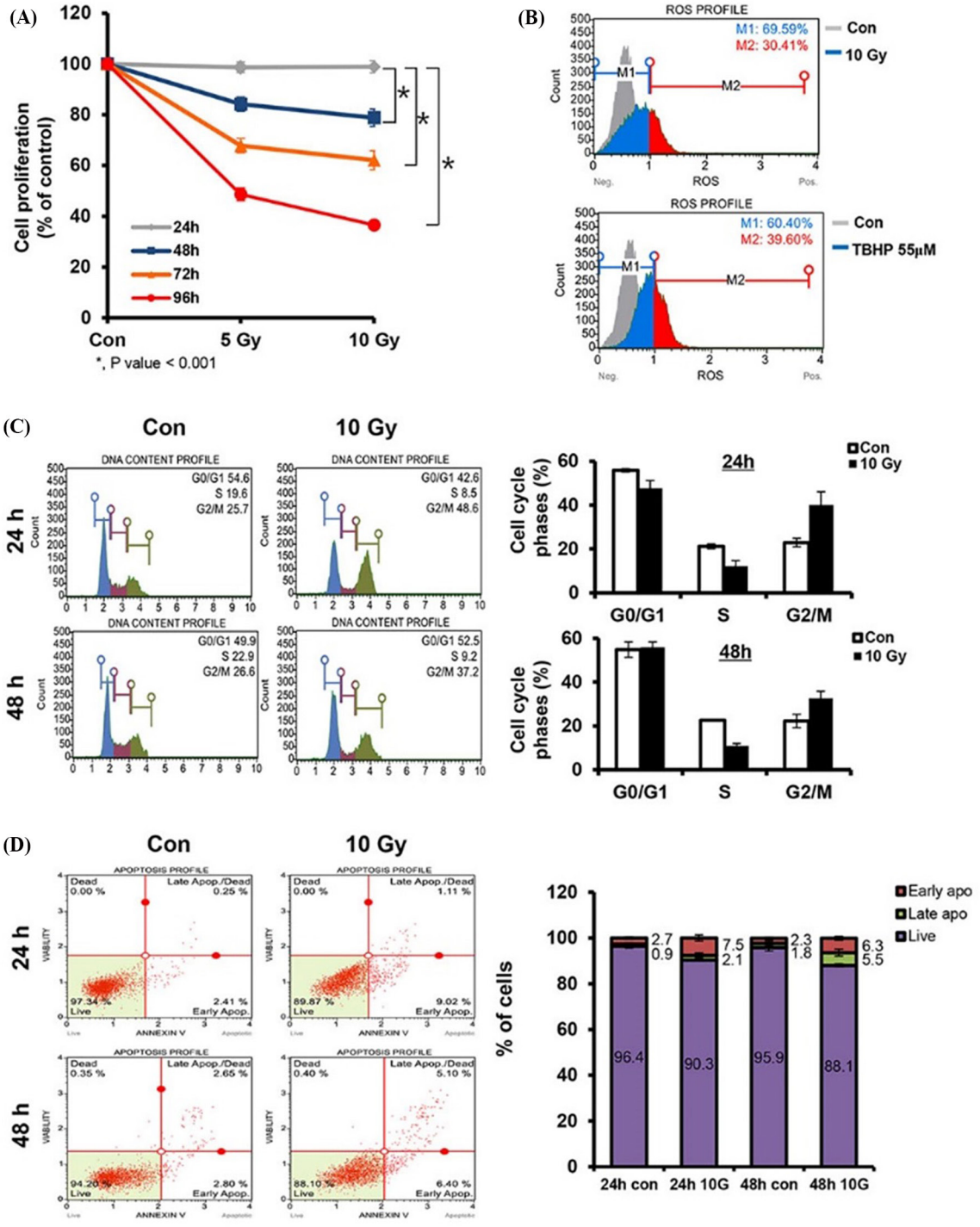

Fig. 1. Induction of growth arrest and ROS accumulation by ionizing radiation in A549 cells. (A) Cell proliferation of A549 was analyzed using MTT assay at different time points after the exposure to IR at 5 and 10 Gy. The bar graph of the results of the MTT assay shows the percentage of viable IR-treated A549 cells. (B) After exposure to 10 Gy IR, A549 cells were quantitatively measured for cellular oxidative stress levels using an oxidative stress reagent assay kit and measured using Muse™ Cell Analyser. Intracellular ROS accumulation is presented as a histogram. The cells treated with TBHP for 4 h were used as a positive control. The blue area (M1) represents the cells with a low level of ROS expression, and the red area (M2) represents the cells with a high level of ROS expression. (C and D) Cell cycle progression and apoptosis of A549 cells were analyzed using the Muse™ Cell Analyser at 24 and 48 h after the exposure of IR (at 10 Gy). The data were obtained from three independent experiments and are shown as mean±standard error of the mean (SEM), *$p<0.001$.

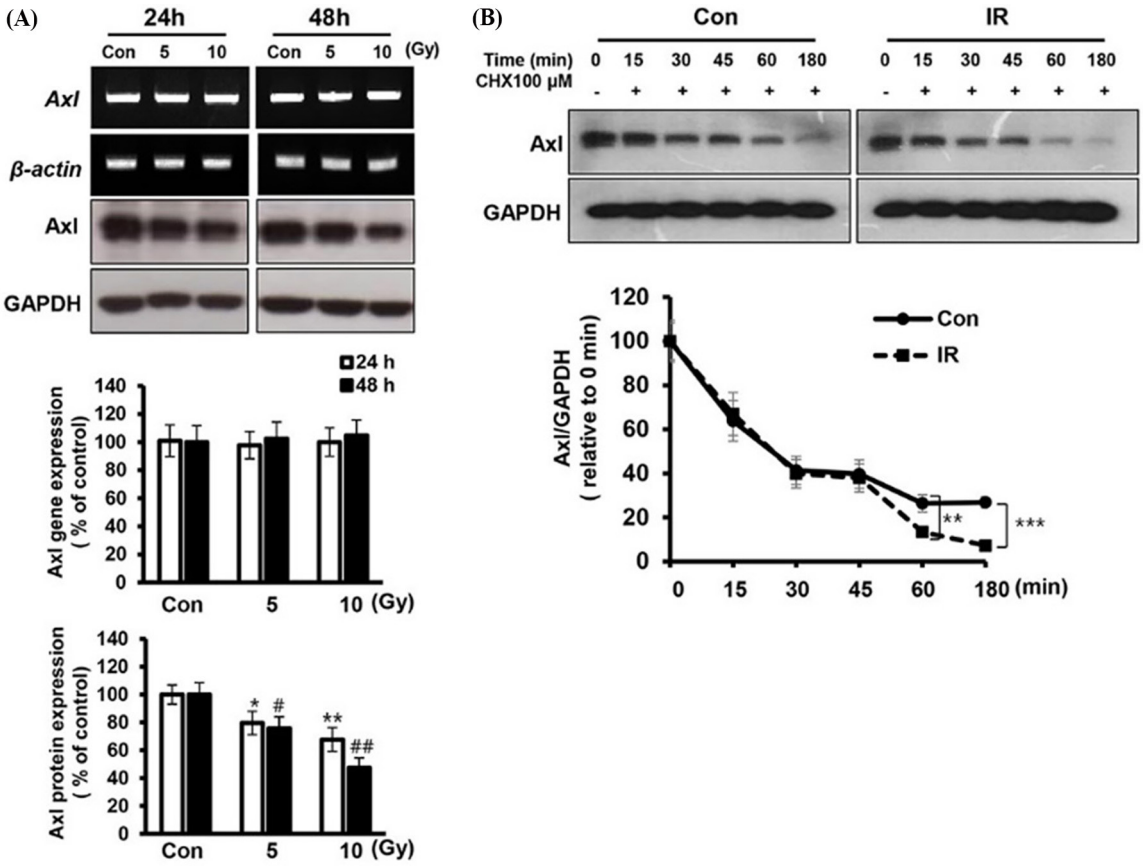

Fig. 2. Induction of Axl protein degradation by ionizing radiation in A549 cells. (A) The gene expression of Axl was analyzed by semiquantitative RT-PCR and the protein expression of Axl was investigated by immunoblot analysis after exposure to IR at 5 and 10 Gy (top). The quantitative graph summarizes the densitometric analysis of three independent experiments showing the Axl gene and protein expression (bottom). Data are presented as the mean±SEM (*$p<0.05$; **$p<0.001$ compared to 24 h control; $^{\#}p<0.05$, $^{\#\#}p<0.01$ compared with 48 h control). (B) A549 cells were treated with cycloheximide (CHX; 100 μM) for the indicated times after the exposure to IR at 10 Gy, and the protein expression of Axl was analyzed by immunoblotting (top). The graph shows data presented as the mean±SEM (**$p<0.01$; ***$p<0.001$). Data are representative of three independent experiments (bottom panel).

the lysosomal pathway, and not through the proteasomal pathway. The visual assessment revealed morphological changes and large autophagic vacuoles in A549 cells following exposure to IR (Fig. 5A). In light of these observations, we further investigated the protein expression of the autophagy molecule, LC3B, to evaluate the role of the autophagolysosomal pathway in the protein degradation of Axl following IR exposure. As shown in Fig. 5B, the protein expression of Axl was reduced following exposure to IR for 48 h compared to control. Further, autophagosome accumulation, as demonstrated by an increased LC3B-II/LC3B-I ratio, was also elevated over time following IR. To further explore the effect of IR on autophagolysosomal pathway-mediated degradation of Axl protein, we used fluorescence microscopy to follow the fate of GFP-LC3B-bound vesicles and RFP-Axl protein after IR. We first determined that the co-localization of GFP-LC3 puncta and RFP-Axl protein was markedly increased in the A549 cells following IR exposure after blocking the lysosomal pathway. Collectively, our data suggest that IR exposure increased Axl protein degradation in lung adenocarcinoma cells through the autophagolysosomal pathway.

4. Discussion

Axl is well-known for its oncogenic effect in NSCLCs [11-15]. Since Axl is considered to be an effective target in several tumours, several attempts to inhibit the protein expression of Axl are currently in progress to treat cancer patients. Although

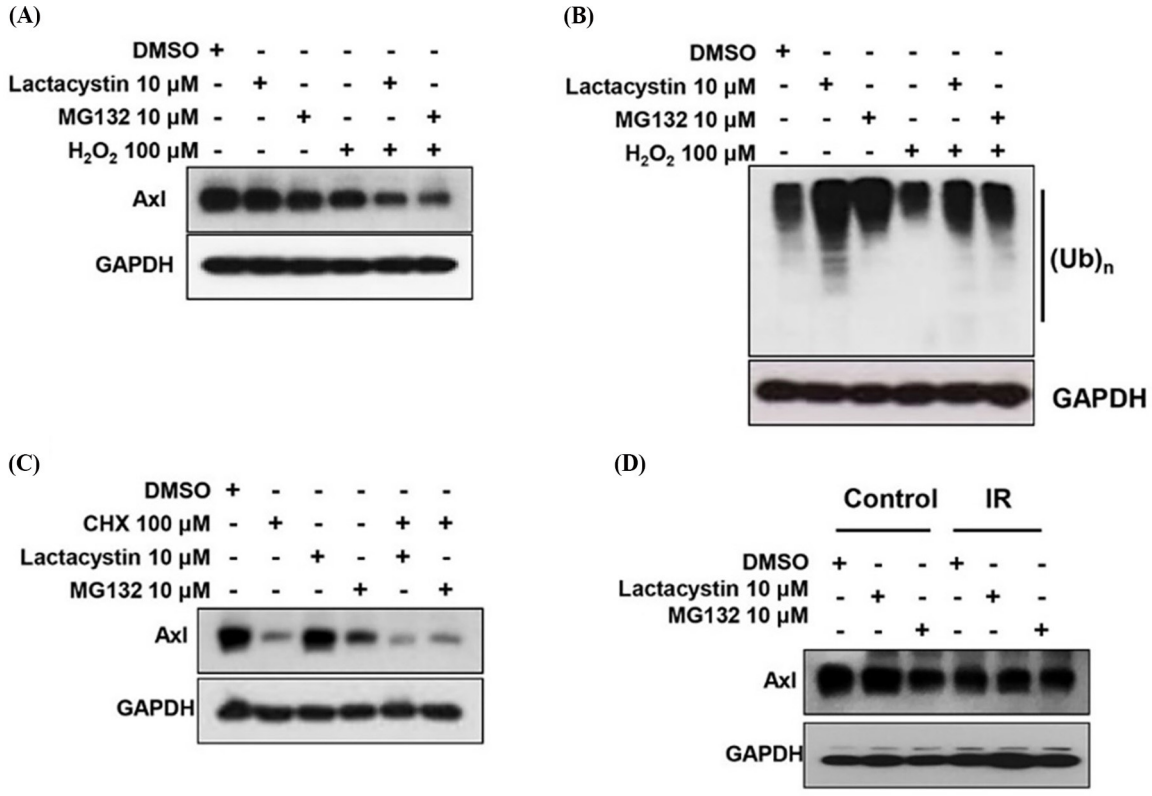

Fig. 3. Assessment of protein degradation of Axl through the proteasomal pathway in ionizing radiation-induced A549 cells. After pretreatment with 10 μM of lactacystin and MG132 for 1 h, A549 cells were treated with 100 μM of H_2O_2 for 3 h. The protein expression of (A) Axl and (B) ubiquitin were analyzed using immunoblotting. (C and D) After pretreatment of A549 cells with the same doses of the indicated inhibitors for 1 h, the cells were treated with 100 μM of CHX for 3 h and IR at 10 Gy. The data are representative of three independent experiments.

IR is a well-accepted standard treatment modality in lung cancer, the molecular events that regulate IR-mediated Axl expression remain unknown. Here, we provide the first evidence that IR induces the degradation of Axl protein through the autophagolysosomal pathway.

In the present study, we demonstrate that IR induces downregulation of the Axl protein level without altering its mRNA levels (Fig. 2). In addition, it was shown that the half-life of Axl protein was reduced in IR-exposed A549 cells compared with control. Thus, our data suggest that there exists a specific pathway for IR-mediated Axl protein degradation.

Our findings showed that proteasomal inhibitors such as MG132 and lactacystin did not affect the restoration of Axl protein in H_2O_2- and IR-treated cells (Fig. 3). These results demonstrated that IR-mediated Axl protein degradation was not associated with the proteasomal degradation pathway. In the present study (Fig. 3), MG132 supplementation resulted in a slight decrease in Axl protein expression. A recent study has suggested that the proteasome inhibitor, MG132, could induce autophagy [32]. This finding was somewhat unexpected but maybe a consequence of the function of MG132-activated autophagy.

IR generates hydroxyl radicals (•OH) and induces radiation-induced cell death by causing DNA damage [33]. Hydrogen peroxide can induce a large number of single-strand breaks, mimicking the effect of IR [34]. In the present study, we also used hydrogen peroxide as the common mediator of DNA damage induction resulting from OH radicals.

Recent studies reported that the autophagy system could be induced by IR and led to the induction of cancer cell death in response to radiation [35,36]. Consistent with these findings, we found that the formation of autophagic vacuoles was visible in the IR-treated A549 cells after 48 h, and the degradation of Axl protein by IR and H_2O_2 was restored after treatment with CQ, a known autophagy inhibitor (Fig. 4, 5). Furthermore, it was observed that the Axl protein expression did not increase over time in IR-treated cells compared with control cells, and it was notably correlated with the increase of the ratio of LC3B-II to LC3B-I in a time-dependent manner. Together, these results

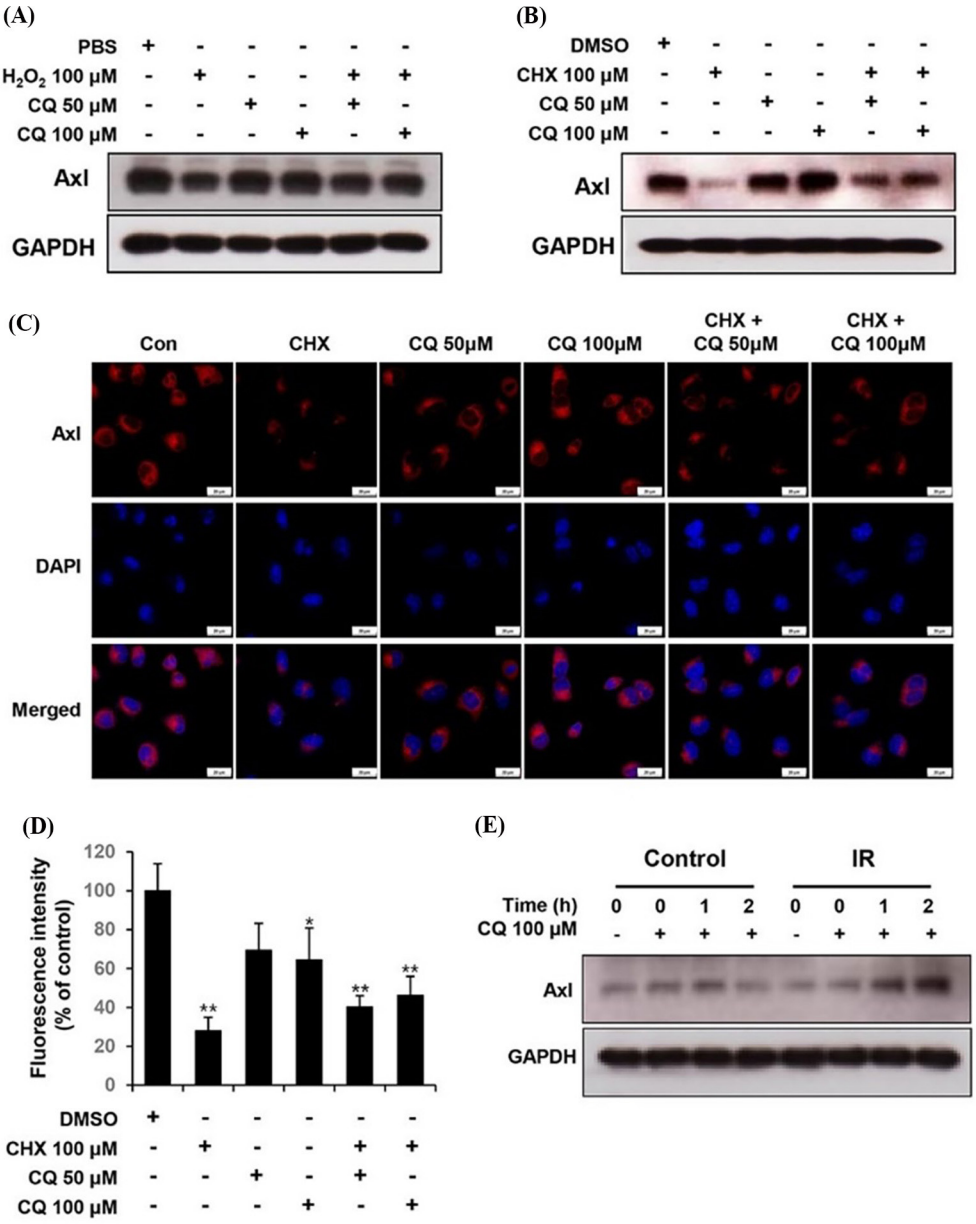

Fig. 4. Assessment of protein degradation of Axl through the lysosomal pathway in ionizing radiation-induced A549 cells. (A and B) After pretreatment with 50 or 100 μM of CQ for 1 h, A549 cells were treated with 100 μM of H_2O_2 and CHX for 3 h. The level of Axl protein was analyzed using immunoblotting. (C) The expression of Axl was evaluated using immunofluorescence analysis after treatment with the indicated reagents. Scale bars, 20 μm. (D) The graph displayed fluorescence intensity (Axl) of treated cells versus control cells. Bars represented mean±SEM from n=3 separate experiments; *$p<0.05$, **$p<0.001$ compared with control (Student t test). (E) After pretreatment with 100 μM of CQ for 1 h, A549 cells were exposed to 10 Gy IR. The level of Axl protein was analyzed after 0, 1, or 2 h by immunoblot analysis. The data are representative of three independent experiments.

indicated that IR-induced Axl degradation is involved in autophagy.

Recent studies have demonstrated that the autophagic cell death pathway could modulate IR sensitivity. The combined treatment with autophagy-inducing reagents and IR enhanced the cytotoxicity of radiation *in vivo* and *in vitro* models of lung cancers and led to cancer radiosensitivity [37-39]. Our studies provided evidence that Axl oncogene may be degraded through autophagy following IR. These data raise the interesting possibility that a combination of autophagy inducer and IR could in-

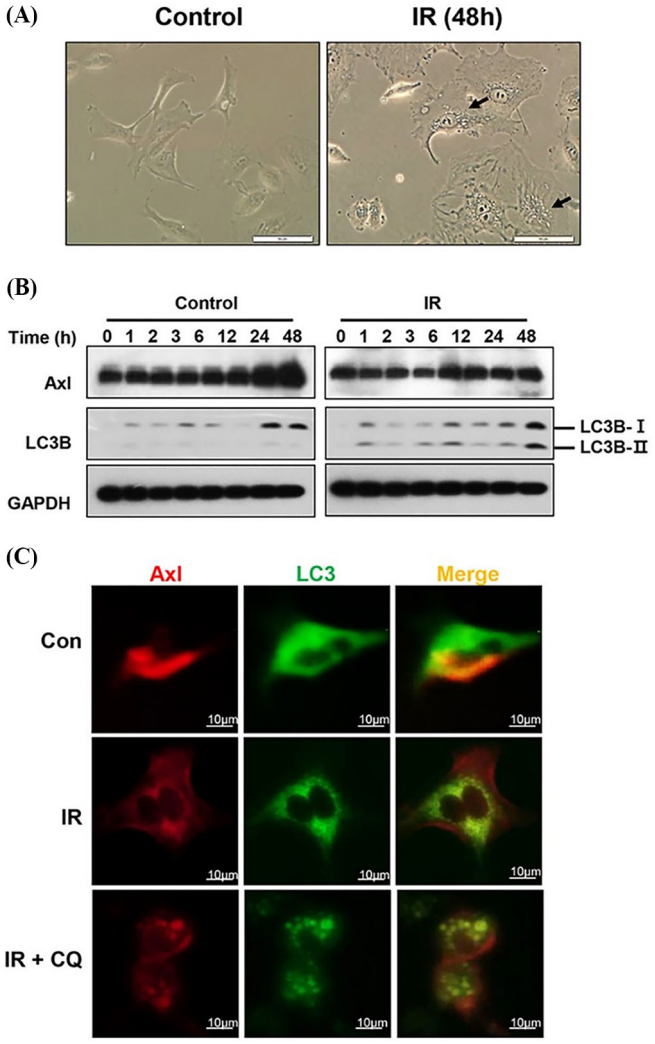

Fig. 5. Ionizing radiation-induced protein degradation of Axl through the autophagy-lysosomal pathway in A549 cells. (A) Visual assessment of A549 cells using microscopic images (magnification=40 x) after the exposure to IR for 48 h. Scale bars, 50 μm. The black arrows show autophagic vacuoles. (B) The protein expression of Axl, LC3B-I, and LC3B-II were analyzed using immunoblotting after exposure to IR for indicated times. (C) The vesicular co-localization of Axl and LC3 was investigated using immunofluorescence analysis after the exposure to IR for 48 h, treated with or without CQ. The data are representative of three independent experiments.

duce more dramatic downregulation of Axl protein in response to IR. However, the possibility of whether autophagy-mediated Axl degradation by IR is sufficient for the radio- and chemo-resistant tumour cells remains to be further investigated. There were a few limitations of this study had. For example, the A549 NSCLC cell line was selected to determine the mechanism of Axl degradation following IR. The use of various tumor cell lines could have improved our experimental evidence to reduce the bias of the cell line selection. In this study, we examined the autophagolysosomal pathway of Axl protein degradation for 48 h, although a long-term study would be helpful for understanding the Axl degradation mechanism and the recurrence of tumor growth in therapeutic approaches using IR. Furthermore, we demonstrated the Axl degradation mechanism in an *in vitro* study. We planned to conduct an in vivo study of human or animal model-based lung cancer tissue.

5. Conclusion

In summary, we found that exposure of NSCLC to IR causes a decrease in the expression of Axl protein through the autophagolysosomal degradation pathway. These findings further strengthen the role of IR in cancer therapy and provide important insight as to how to therapeutically modulate Axl.

Acknowldegment

This research was funded by the Ministry of Science, ICT & Future Planning and by the Basic Science Research Programme. It was also supported by a grant from the National Research Foundation of Korea (NRF), funded by the Ministry of Science and ICT (grant number: RS-2025-02613113).

References

1. Torre LA, Siegel RL, Ward EM and Jemal A. 2016. Global cancer incidence and mortality rates and trends—an update. *Cancer Epidemiol. Biomarkers Prev.* **25**(1):16-27. https://doi.org/10.1158/1055-9965.EPI-15-0578.
2. Oser MG, Niederst MJ, Sequist LV and Engelman JA. 2015. Transformation fromnon-small-cell lung cancer to small-cell lung cancer: molecular drivers and cells of origin. *Lancet Oncol.* **16**(4):e165-e72. https://doi.org/10.1016/S1470-2045(14)71180-5.
3. Salama JK and Vokes EE. 2013. New radiotherapy and chemoradiotherapy approachesfor non-small-cell lung cancer. *J. Clin. Oncol.* **31**(8):1029-1038. https://doi.org/10.1200/JCO.2012.44.5064.
4. Linger RM, Keating AK, Earp HS and Graham DK. 2008. TAM receptor tyrosinekinases: biologic functions, signaling, and potential therapeutic targeting in human cancer. *Adv. Cancer Res.* **100**:35-83. https://doi.org/10.1016/S0065-230X(08)00002-X.
5. Feneyrolles C, Spenlinhauer A, Guiet L, Fauvel B, Daydé-Cazals B, Warnault P, Cheve G and Yasri A. 2014. Axl kinase as a key target for oncology: focus on small molecule inhibitors. *Mol. Cancer. Ther.* **13**(9):2141-2148. https://doi.org/10.1158/1535-7163.MCT-13-1083.
6. Tirosh I, Izar B, Prakadan SM, Wadsworth MH, Treacy D, Trombetta JJ, Rotem A, Rodman C, Lian C, Murphy G, Fallahi-Sichani

M, Dutton-Regester K, Lin JR, Cohen O, Shah P, Lu D, Genshaft AS, Hughes TK, Ziegler CGK, Kazer SW, Gaillard A, Kolb KE, Villani AC, Johannessen CM, Andreev AY, Van Allen EM, Bertagnolli M, Sorger PK, Sullivan RJ, Flaherty KT, Frederick DT, Jane-Valbuena J, Yoon CH, Rozenblatt-Rosen O, Garraway LA, Golub TR, Getz G, Hacohen N, Patel AP, Mesirov JP, Mesirov JP, Schreiber R, Wargo JA, Raza A, Shalek AK, Regev A and Garraway LA. 2016. Dissecting the multicellular ecosystem of metastatic melanoma by single-cell RNA-seq. *Science*. **352**(6282):189-196. https://doi.org/10.1126/science.aad0501.

7. Hong CC, Lay JD, Huang JS, Cheng AL, Tang JL, Lin MT, Lai GM and Chuang SE. 2008. Receptor tyrosine kinase AXL is induced by chemotherapy drugs and overexpression of AXL confers drug resistance in acute myeloid leukemia. *Cancer Lett.* **268**(2):314-324. https://doi.org/10.1016/j.canlet.2008.04.017.
8. Zhang Z, Lee JC, Lin L, Olivas V, Au V, LaFramboise T, Mohamed AR, Wang W, Levine AD, Rho JK, Choi YJ, Choi CM, Kim SW, Jang SJ, Park YS, Kim WS, Lee DH, Lee JS, Miller VA, Arcila M, Ladanyi M, Moonsamy P, Sawyers C, Boggon TJ, Ma PC, Costa C, Taron M, Rosell R, Halmos B and Bivona TG. 2012. Activation of the AXL kinase causes resistance to EGFR-targeted therapy in lung cancer. *Nat. Genet.* **44**(8):852-860. https://doi.org/10.1038/ng.2330.
9. Müller J, Krijgsman O, Tsoi J, Robert L, Hugo W, Song C, Kong X, Possik PA, Cornelissen-S PDM, Foppen MHG, Kemper K, Goding CR, McDermott U, Blank C, Haanen JBAG, Graeber TG, Lo RS and Peeper DS. 2014. Low MITF/AXLratio predicts early resistance to multiple targeted drugs in melanoma. *Nat. Commun.* 1**5**(5):1-15. https://doi.org/10.1038/ncomms6712.
10. Zhou L, Liu XD, Sun M, Zhang X, German P, Bai S, Ding Z, Tannir N, Wood CG, Matin SF, Karam JA, Tamboli P, Sircar K, Rao P, Rnkin EB, Laird DA, Hoang AG, Walker CL, Giaccia AJ and Jonasch E. 2016. Targeting MET and AXL overcomes resistance to sunitinib therapy in renal cell carcinoma. *Oncogene*. **35**(21):2687-2697. https://doi.org/10.1038/onc.2015.343.
11. Linger RM, Cohen RA, Cummings CT, Sather S, Migdall-Wilson J, Middleton DH, Lu X, Baron AE, Franklin D, Merrick DT, Jedlicka P, DeRyckere D, Heasley LE and Graham DK. 2013, Mer or Axl receptor tyrosine kinase inhibition promotes apoptosis, blocks growth and enhances chemosensitivity of human non-small cell lung cancer. *Oncogene*. **32**(29):3420-3431. https://doi.org/10.1038/onc.2012.355.
12. Iida S, Miki Y, Suzuki T, Mori K, Saito M, Niikawa H, Kondo T, Yamada-O H and Sasano H. 2014. Activation of AXL and antitumor effects of a monoclonal antibodyto AXL in lung adenocarcinoma. *Anticancer Res.* **34**(4):1821-1827.
13. Brand TM, Iida M, Stein AP, Corrigan KL, Braverman CM, Luthar N, Toulany M, Gill PS, Salgia R, Kimple RJ and Wheeler DL. 2014. AXL mediates resistance to cetuximab therapy. *Cancer Res.* **74**(18):5152-5164. https://doi.org/10.1158/0008-5472.CAN-14-0294.
14. Byers LA, Diao L, Wang J, Saintigny P, Girard L, Peyton M, Shen L, Fan Y, Giri U, Tumula PK, Nilsson MB, Gudikote J, Tran H, Cardnell RJG, Bearss DJ, Warner SL, Foulks JM, Kanner SB, Gandhi V, Krett N, Rosen ST, Kim ES, Herbst RS, Blumenschein GR, Lee JJ, Lippman SM, Ang KK, Mills GB, Hong WK, Weinstein JN, Wistuba II, Coombes KR, Minna JD and Heymach JV. 2013. An epithelial-mesenchymal transition gene signature predicts resistanceto EGFR and PI3K inhibitors and identifies Axl as a therapeutic target for overcoming EGFR inhibitor resistance. *Clin. Cancer Res.* **19**(1):279-290. https://doi.org/10.1158/1078-0432.CCR-12-1558.
15. Ishikawa M, Sonobe M, Nakayama E, Kobayashi M, Kikuchi R, Kitamura J, Imamura N and Date H. 2013. Higher expression of receptor tyrosine kinase Axl, and differential expression of its ligand, Gas6, predict poor survival in lung adenocarcinoma patients. *Ann. Surg. Oncol.* **20**(Suppl 3):S467-S476. https://doi.org/10.1245/s10434-012-2795-3.
16. Squatrito M, Brennan CW, Helmy K, Huse JT, Petrini JH and Holland EC. 2010. Loss of ATM/Chk2/p53 pathway components accelerates tumor developmentand contributes to radiation resistance in gliomas. *Cancer cell*. **18**(6):619-629. https://doi.org/10.1016/j.ccr.2010.10.034.
17. Acosta JC and Gil J. 2012. Senescence: a new weapon for cancer therapy. *Trends Cell.Biol.* **22**(4):211-219. https://doi.org/10.1016/j.tcb.2011.11.006.
18. Jackson SP and Bartek J. 2009. The DNA-damage response in human biology and disease. *Nature*. **461**(7267):1071-1078. https://doi.org/10.1038/nature08467.
19. Bentzen SM. 2006. Preventing or reducing late side effects of radiation therapy: radiobiology meets molecular pathology. *Nat. Rev. Cancer.* **6**(9):702-713. https://doi.org/10.1038/nrc1950.
20. Moynahan ME and Jasin M. 2010. Mitotic homologous recombination maintains genomicstability and suppresses tumorigenesis. *Nat. Rev. Mol. Cell. Biol.* **11**(3):196-207. https://doi.org/10.1038/nrm2851.
21. Ciccia A and Elledge SJ. 2010. The DNA damage response: making it safe to play with knives. *Mol. Cell.* **40**(2):179-204. https://doi.org/10.1016/j.molcel.2010.09.019.
22. Khanna A. 2015. DNA damage in cancer therapeutics: a boon or a curse? *Cancer Res.* **75**(11):2133-2138. https://doi.org/10.1158/0008-5472.CAN-14-3247.
23. Olive PL and Durand RE. 1997. Apoptosis: an indicator of radiosensitivity in vitro? *Int.J. Radiat. Biol.* **71**(6):695-707. https://doi.org/10.1080/095530097143707.
24. Shinomiya N. 2001. New concepts in radiation-induced apoptosis:'premitotic apoptosis'and 'postmitotic apoptosis'. *J. Cell Mol. Med.* **5**(3):240-253. https://doi.org/10.1111/j.1582-4934.2001.tb00158.x.
25. Nagelkerke A, Bussink J, Geurts-Moespot A, Sweep FC and Span PN. 2015. Therapeutic targeting of autophagy in cancer. Part II: pharmacological modulation of treatment-induced autophagy. *Seminars in cancer biology* **31**:99-105. https://doi.org/10.1016/j.semcancer.2014.06.001.
26. Mizushima N, Ohsumi Y and Yoshimori T. 2002. Autophagosome formation in mammalian cells. *Cell Struct. Funct.* **27**(6):421-429. https://doi.org/10.1247/csf.27.421.
27. Lee EH, Park CH, Choi HJ, Kawala RA, Bai HW and Chung BY. 2018. Dexamethasone modified by gamma-irradiation as a novel anticancer drug in human non-small cell lung cancer. *PloS one*. **13**(4):e0194341. https://doi.org/10.1371/journal.pone.0194341.
28. Kawala RA, Ramadhani FJ, Choi HJ, Lee EH, Park CH, Chung BY and Bai HW. 2019. Kenalog modified by ionizing radiation induces intrinsic apoptosis mediated by elevated levels of reactive oxygen species in melanoma cancer. *Oncol. Rep.* **41**(3):1837-1850. https://doi.org/10.3892/or.2018.6940.
29. Shieh YS, Lai CY, Kao YR, Shiah SG, Chu YW, Lee HS and Wu CW. 2005. Expression of axl in lung adenocarcinoma and correlation with tumor progression. *Neoplasia*. **7**(12):1058-1064. https://doi.org/10.1593/neo.05640.

30. Lee EH, Ji KY, Kim EM, Kim SM, Song HW, Choi HR, Chung BY, Choi HJ, Bai HW and Kang HS. 2017. Blockade of Axl signaling ameliorates HPV16E6-mediated tumorigenecity of cervical cancer. *Sci. Rep*. **7**(1):5759. https://doi.org/10.1038/s41598-017-05977-8.
31. Wang X and Robbins J. 2014. Proteasomal and lysosomal protein degradation and heart disease. *J. Mol. Cell. Cardiol*. **71**:16-24. https://doi.org/10.1016/j.yjmcc.2013.11.006.
32. Wang D, Xu Q, Yuan Q, Jia M, Niu H, Liu X, Zhang J, Young CY and Yuan H. 2019. Proteasome inhibition boosts autophagic degradation of ubiquitinated-AGR2 and enhances the antitumor efficiency of bevacizumab. *Oncogene*. **38**(18):3458-3474. https://doi.org/10.1038/s41388-019-0675-z.
33. Azzam EI, Jay-Gerin JP and Pain D. 2012. Ionizing radiation-induced metabolic oxidative stress and prolonged cell injury. *Cancer Lett.* **327**(1-2):48-60. https://doi.org/10.1016/j.canlet.2011.12.012.
34. Driessens N, Versteyhe S, Ghaddhab C, Burniat A, De Deken X, Van Sande J, Dumont JE, Miot F and Corvilain B. 2009. Hydrogen peroxide induces DNA single-and double-strand breaks in thyroid cells and is therefore a potential mutagen for this organ. *Endocr.-Relat. Cancer.* **16**(3):845-856. https://doi.org/10.1677/ERC-09-0020.
35. Ito H, Daido S, Kanzawa T, Kondo S and Kondo Y. 2005. Radiation-induced autophagyis associated with LC3 and its inhibition sensitizes malignant glioma cells. *Int. J. Oncol.* **26**(5):1401-1410. https://doi.org/10.3892/ijo.26.5.1401.
36. Kuwahara Y, Oikawa T, Ochiai Y, Roudkenar M, Fukumoto M, Shimura T, Ohtake Y, Ohkubo Y, Mori S, Uchiyama Y and Fukumoto M. 2011. Enhancement of autophagy is a potential modality for tumors refractory to radiotherapy. *Cell Death Dis.* **2**(6):e177. https://doi.org/10.1038/cddis.2011.56.
37. Peng PL, Kuo WH, Tseng HC and Chou FP. 2008. Synergistic tumor-killing effect of radiation and berberine combined treatment in lung cancer: the contribution of autophagic cell death. *Int. J. Radiat. Oncol. Biol. Phys.* **70**(2):529-542. https://doi.org/10.1016/j.ijrobp.2007.08.034.
38. Kim KW, Hwang M, Moretti L, Jaboin JJ, Cha YI and Lu B. 2008. Autophagy upregulation by inhibitors of caspase-3 and mTOR enhances radiotherapy in a mouse model of lung cancer. *Autophagy.* **4**(5):659-668. https://doi.org/10.4161/auto.6058.
39. Kim KW, Speirs CK, Jung DK and Lu B. 2011. The zinc ionophore PCI-5002 radiosensitizes non-small cell lung cancer cells by enhancing autophagic cell death. *J. Thorac.Oncol.* **6**(9):1542-1552. https://doi.org/10.1097/JTO.0b013e3182208fac.